Electronic Structure and Photochemical Interconversions of Dihydropentalene Radical Cations

Thomas Bally,*,† Leo Truttmann,†,§ Jih Tzong Wang,‡ and Ffrancon Williams*,‡

Contribution from the Institute of Physical Chemistry, University of Fribourg, Pérolles, CH-1700 Fribourg, Switzerland, and the Department of Chemistry, University of Tennessee, Knoxville, Tennessee 37996-1600

Received March 15, 1995[⊗]

Abstract: Starting from the recently characterized radical cation of bicyclo[3.3.0]octa-2,6-diene-4,8-diyl, four additional dihydropentalene radical cations (DHP$^{\bullet+}$) can be formed by phototautomerization in Freon glasses and argon matrices where they can be characterized by optical (Freon, argon) and ESR spectroscopy (Freon). Two of these DHP isomers can be prepared independently, while the cations of the other two are identified by analogy of their spectra with those of related compounds. The electronic structure of 1,2-, 1,4-, and 1,5-DHP$^{\bullet+}$, which have linear and cross-conjugated triene π-systems is discussed on the basis of their photoelectron and optical spectra and INDO/S calculations. The part of the $C_8H_8^{\bullet+}$ potential surface comprising all ten possible DHP$^{\bullet+}$ tautomers and some related valence isomers is explored by high-level ab initio calculations. An FMO-based set of rules for sigmatropic rearrangements in radical cations is presented and serves to rationalize the observed H-shifts.

1. Introduction

In their comprehensive study on the electronic structure of aromatic radical ions, Shida and Iwata had noted in 1972 that the radical cation of cyclooctatetraene (COT$^{\bullet+}$) undergoes an interesting two-step photoreaction leading eventually to a species with an electronic absorption (EA) spectrum which bears no resemblance to that of COT$^{\bullet+}$ and therefore indicated to them "a rather drastic change involving a rearrangement of the carbon skeleton".[1] We have recently been able to elucidate the identities of the primary[2] and the secondary photoproduct of COT$^{\bullet+}$,[3] both being formally tautomeric dihydropentalene radical cations (DHP$^{\bullet+}$).

In the preceding paper[4] we discussed in some detail the formation of the primary product, 3a,6a-DHP$^{\bullet+}$, photochemically from COT$^{\bullet+}$ as well as thermally from semibullvalene. During our investigation of the second photoproduct[3] which arises from 3a,6a-DHP$^{\bullet+}$, we discovered that this in turn undergoes further phototransformations to at least two other products which can be interconverted reversibly with the former and are hence thought to be also DHP$^{\bullet+}$ tautomers. This paper gives a full account of these results and presents a theoretical framework within which these transformations can be viewed.

The thermal chemistry of *neutral* DHP has been explored in some detail by several groups. In particular, Meier et al. recently succeeded to characterize the unstable isomers 1,4- and 1,6-DHP and elaborated optimal conditions for a preparation of the two well-known stable 1,2- and 1,5-DHP by pyrolysis of COT.[5a,b] They also studied thermal rearrangements between different DHP isomers and found that both formally allowed ([1,5]) and forbidden ([1,3] and [1,6]) sigmatropic hydrogen shifts seem to participate in the observed overall processes.[5c]

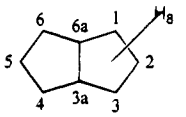

DHP

Since radical ion rearrangements follow laws which are often quite different from those prevailing in their neutral counterparts and because additional isomers which have no stable equivalent on the neutral hypersurface often need to be considered we wish to start out by presenting a general scheme of all possible DHP tautomers (Scheme 1). Due to the multitude of possible

Scheme 1. All Possible Stable DHP$^{\bullet+}$ Tautomers and Their Interconversion Pathways[a]

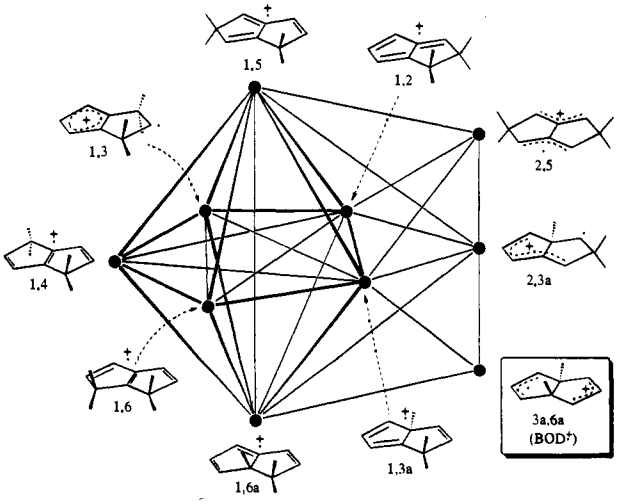

[a] Each line represents a single H-shift. Note that seven of the ten isomers are arranged in a pentagonal bipyramid.

† Institute of Physical Chemistry, University of Fribourg.
‡ Department of Chemistry, University of Tennessee.
§ Present address: Department of Chemistry, California Institute of Technology, Pasadena, CA 91125.
⊗ Abstract published in *Advance ACS Abstracts*, July 1, 1995.

(1) Shida, T.; Iwata, S. *J. Am. Chem. Soc.* **1973**, *95*, 3473.
(2) (a) Dai, S.; Wang, J. T.; Williams, F. *J. Am. Chem. Soc.* **1990**, *112*, 2835. (b) Dai, S.; Wang, J. T.; Williams, F. *J. Am. Chem. Soc.* **1990**, *112*, 2837.
(3) Bally. T.; Truttmann, L.; Dai, S.; Wang, J. T; Williams. F. *Chem. Phys. Lett.* **1993**, *212*, 141.
(4) Bally. T.; Truttmann, L.; Dai, S.; Williams, F. *J. Am. Chem. Soc.* **1995**, *117*, 7916.
(5) (a) Meier, H.; Pauli, A.; Kolshorn, H.; Kochhan, P. *Chem. Ber.* **1987**, *120*, 1607. (b) Meier, H.; Pauli, A.; Kochhan, P. *Synthesis* **1987**, 573. (c) Pauli, A.; Kolshorn, H.; Meier, H. *Chem. Ber.* **1987**, *120*, 1611.

0002-7863/95/1517-7923$09.00/0

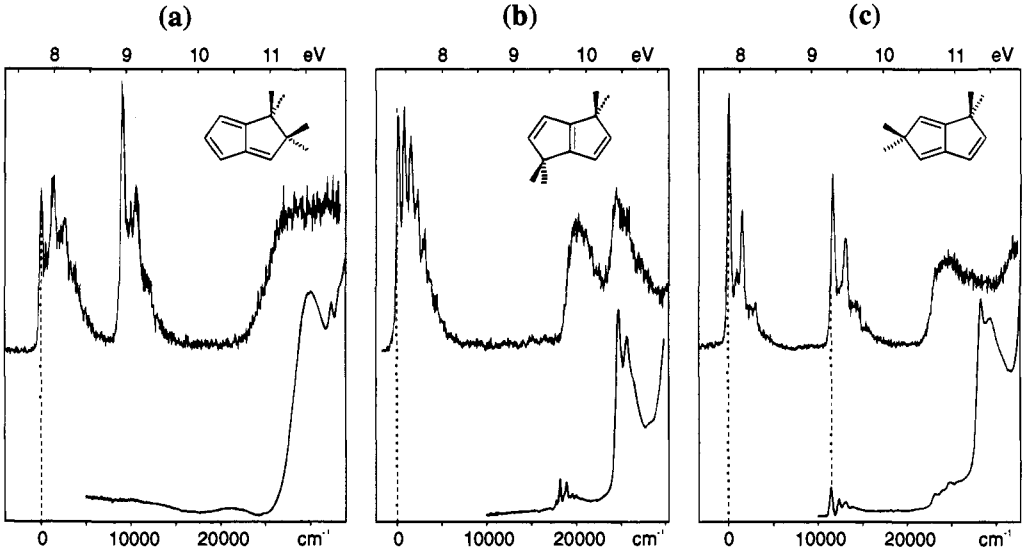

Figure 1. Photoelectron (PE) spectra of 1,2-, 1,4-, and 1,5-DHP and electronic absorption (EA) spectra of the corresponding radical cations in Freon glasses. The two sets of spectra are plotted on the same energy scale (PE spectra in eV, EA spectra in wavenumbers) whereby the origin of the EA spectra is placed into the 0−0 transition of the first PE band (=energy of ground-state radical cation).

interconversions we found it most convenient to represent the seven *m,n*-tautomers that are all interconnected by single H-shifts (i.e. for which $m = 1$ and $n = 2$, 3, 3a, 4, 5, 6, and 6a) in the form of a pentagonal bipyramid, whereas the remaining species are situated on three external points. All lines connecting dots in Figure 1 can be associated with single [1,*j*] hydrogen shifts where *j* is equal to 2 (10 lines), 3 (13 lines) or 4 (7 lines). Furthermore, some of the tautomers (1,2-, 1,3a-, 1,5-, 1,6a-, and 2,3a-DHP$^{\bullet+}$) can undergo narcissistic rearrangements leading back to the original molecule. Scheme 1 will serve as a basis in our attempts to identify the various photoporoducts which we observed in the course of our experiments described below.

2. Experimental and Theoretical Methods

(a) Syntheses. Semibullvalene (which upon ionization yields 3a,6a-DHP$^{\bullet+}$)[2a] was made by gas-phase photolysis of cyclooctatetraene (Fluka, purum) according to Turro et al.[6] 1,5-DHP was produced by cyclization of 6-vinylfulvene which was generated in situ by flash vacuum pyrolysis of its Diels−Alder adduct with cyclopentadiene according to Griesbeck.[7] We attempted to mimic exactly the experimental conditions of Griesbeck (30 cm empty quartz tube, 0.01 Torr pressure, temperature of precursor 80−120 °C), but we were unable to detect the less stable 1,6a- and 1,3a-DHPs at any oven temperature between 300 °C (very little reaction) and 500 °C (highest yield of 1,5-DHP). Instead, the 1,5-DHP formed in this temperature range was always accompanied by another product which fortuitiously turned out to be 1,4-DHP by ^{1}H and ^{13}C-NMR[5a] (very small amounts of 1,6-DHP could also be detected in the pyrolysate). 1,2-DHP was prepared by passing the crude pyrolysate (containing mainly 1,5-DHP) over a basic alumina column as described by Meier.[5b] All three DHPs were isolated in pure form by preparative gas chromatography on β,β'-oxydipropionitrile (30% on Chromosorb W, 400 cm, 40−60 °C).

(b) Procedures. Freon Glasses. Solutions ($\approx 10^{-2}$ M) of the neutral precursors in $CFCl_2CFCl_2$ (FC-112), CF_2ClCCl_3 (FC-112a), $CF_2ClCFCl_2$ (FC-113), CF_3CCl_3 (FC-113a) for ESR measurements or in a 1:1 mixture of $CFCl_3$ (FC-11) and CF_2BrCF_2Br (FC-114B2) for optical studies[8] were degassed and filled into quartz tubes (ESR work) or special optical cuvettes[9] where they were γ-irradiated at 77 K with a dose of ≈0.2 Mrad (ESR work) or ≈0.5 Mrad (optical work) in a ^{60}Co source (Gammacell). All ESR measurements were carried out on a Bruker ER 200 D SRC spectrometer (TE_{102} cavity, ER-4102-ST X-band resonator, 35 dB microwave power) equipped with variable-temperature accessories. Optical spectra were recorded at 77 K on a modified PE Lambda 9 instrument[9] under computer control.

Photolyses. For the ESR work, light from a tungsten lamp was filtered at $\lambda = 410$ nm (narrow 380−450 nm bandpass filter), $\lambda > 640$ nm (Corning Filter C. S. No. 2-64), or $\lambda > 840$ nm (Corning Filter C. S. No. 7-56). In the optical work, light from a 1 kW Argon plasma lamp was passed through a home-built monochromator ($\lambda = 400$ nm), interference filters ($\lambda = 450$ and 800 nm), or cutoff filters ($\lambda > 540$ and >630 nm).

Argon Matrices. Mixtures ≈1000:1:1 of argon, CH_2Cl_2, and the neutral substrate were deposited at ≈20 K on a CsI window (≈2 mMol argon). After deposition the sample was cooled to the lowest temperature attainable by the closed-cycle cryostat (Air Products CSW 200) and exposed to X-rays (40 kV/40 mA, tungsten anode) during 90 min. Details of the technique are described in ref 9.

Photoelectron Spectra. PE spectra were recorded on a modified PE 16 instrument containing a preretardation device.[10] Calibration was effected with Xe and trace water. Resolution at the Xe peaks (and in preretardation mode in the entire spectrum) was 22 meV.

(c) Quantum-Chemical Calculations. As (semiempirical or ab initio) UHF wave functions of the different DHP tautomers show varying (and sometimes high) degrees of spin contamination, all SCF calculations were done with the ROHF procedure. Geometries were optimized at the SCF/6-31G* level with GAMESS,[11] while correlation effects were accounted for by single-point calculations with the RMP2 procedure[12] using GAUSSIAN 92.[13] The spectroscopic properties were calculated at the same geometries by the INDO/S-CI method[14a] (based

(6) Turro, N. J.; Liu, J.-M.; Zimmerman, H. E.; Factor, R. E. *J. Org. Chem.* **1980**, *45*, 3511.

(7) Griesbeck, A. *J. Org. Chem.* **1989**, *54*, 4981. Griesbeck, A. *Synthesis*, **1990**, 144.

(8) Sandorfy, C. *Can. J. Spectrosc.* **1965**, *85*, 10. Grimison, A.; Simpson, G. A. *J. Phys. Chem.* **1968**, *72*, 1776.

(9) Bally, T. in *Radical Ionic Systems*; Kluwer Academic Press: Dordrecht, 1991; Chapter 1.

(10) Dressler, R.; Neuhaus, L.; Allan, M. *J. Electron Spectrosc. Relat. Phenom.* **1983**, *31*, 181.

(11) (a) Gamess, Schmidt, M. W.; Baldridge, K. K.; Boatz, J. A.; Jensen, J. H.; Koseki, S.; Gordon, M. S.; Nguyen, K. A.; Windus T. L. ; Elbert, S. T. *QCPE Bull.* **1990**, *10*, 52. (b) For the version used in this work see Schmidt, M. W.; Baldridge, K. K.; Boatz, J. A.; Elbert, S. T.; Gordon, M. S.; Jensen, J. H.; Koseki, S.; Matsanuga, N. ; Nguyen, K. A.; Su, S. J.; Windus, T. L.; Dupuis M.; Montgomery, J. A. *J. Comp. Chem.* **1993**, *14*, 1347.

(12) Knowles, P. J.; Andrews, J. S.; Amos, R. D.; Handy, N. C.; Pople, J. A. *Chem. Phys. Lett.* **1991**, *186*, 130. This method is implemented (but not documented) in the GAUSSIAN92 program[13] where it can be invoked with the ROMP2 keyword. The RMP2 energies published by Knowles et al. were reproduced to 10^{-7} hartree.

(13) Frisch, M. J.; Trucks, G. W.; Head-Gordon, M.; Gill, P. M. W.; Wong, M. W.; Foresman, J. B.; Johnson, B. G.; Schlegel, H. B.; Robb, M. A.; Replogle, E. S.; Gomperts, R.; Andres, J. L.; Raghavachari, K.; Binkley, J. S.; Gonzales, C.; Martin, R. L.; Fox, D. J.; DeFrees, D. J.; Baker, J.; Stewart, J. J. P.; Pople, J. A. Gaussian, Inc., Pittsburgh, PA, 1992.

also on ROHF wave functions[14b]) with the ZINDO program.[14c] ESR hyperfine coupling constants were also evaluted at the ab initio geometries by the standard INDO[15] or by the AM1 procedure.[16]

3. Results and Discussion

(a) Electronic Spectra and Electronic Structure of 1,2-1,4-, and 1,5-DHP$^{\bullet+}$. In Figure 1a–c we present the photoelectron (PE) spectra of 1,2-, 1,4-, and 1,5-DHP as well as the electronic absorption (EA) spectra of the corresponding radical cations (drawn to scale with the PE spectra), while a schematic representation of the excited state energies from the experiments and from INDO/S calculations is given in Figure 2a–c. Table 1 lists the energies of the different ionic states next to calculated values.

1,2-DHP$^{\bullet+}$. Starting with this *pentafulvene*-type hydrocarbon, we note that the PE spectrum shows two well-separated bands from π-ionizations at energies which are very similar to those of related dimethylfulvene ($I_{v,1}$ = 8.06 eV, $I_{v,2}$ = 8.75 eV)[17] followed by a large gap before the onset of σ-ionizations at ≈11 eV. The EA spectrum shows no distinct features below 25 000 cm^{-1} in spite of the fact that INDO/S predicts transitions to three electronic states (albeit with very low oscillator strengths) in this region.[18] In particular, we find no sharp EA-band which coincides with the second PE band, as it is often found in other polyenic hydrocarbon cations.[19] The other two states which are predicted to lie in the gap of the PE spectrum are of "non-Koopmans" (NK) type[20a] and are therefore not expected to contribute to the PE spectrum.[20b] The intense EA band at ≈30 000 cm^{-1} probably corresponds to excitation into one of the highly mixed NK states predicted at 4.40 and 4.78 eV (35 500 and 38 560 cm^{-1}) by INDO/S.

A noteworthy feature of 1,2-DHP is the pronounced relaxation energy (0.41 eV by ROHF/6-31G*) of the radical cation which is accompanied by strong bond length changes in the cyclopentadiene ring (see Figure 10). As a consequence of the 0.86 eV shift in ϵ_{HOMO} between the neutral and the cation geometry (6-31G*/SCF), INDO/S predicts a blue shift of 0.56 eV for the first excited state upon relaxation of the cation (see Figure 2a) such that no coincidence between the second PE and the first EA band is expected. Unfortunately we cannot verify this interesting prediction due to the small oscillator strength of the electronic transition. The next two excited states which are of predominant non-Koopmans character undergo smaller shifts while the strong UV-transitions are almost unaffected by the cation relaxation.

1,4-DHP$^{\bullet+}$. Turning to this isomer with a *linear conjugated triene* π-chromophore,[19] we have already pointed out previously the evident similarity of its EA spectrum to that of hexatriene radical cation (HT$^{\bullet+}$) which had actually led us to the identification of this species as the primary photoproduct of 3a,6a-DHP$^{\bullet+}$.[3] INDO/S predicts the shifts of both EA bands between HT$^{\bullet+}$ and 1,4-DHP$^{\bullet+}$ with the correct sign but underestimates them (cf. Table 2). Interestingly, we notice a significant displacement of the first EA band relative to the second PE band which is uncommon for linear conjugated polyenes. It indicates that the energy of the first excited state is lowered upon relaxation of the cation from the neutral geometry. This is corroborated by INDO/S which predicts a 0.21 eV red shift of the $1^2A_u \rightarrow 1^2B_g$ transition on going from the neutral to the cation geometry.

With regard to the second band in the EA spectrum which coincides with the second PE band, we note that INDO/S predicts two states (2^2B_g and 2^2A_u) which are nearly degenerate and at similar energy at both geometries. Whereas, due to dipole selection rules, the strong EA band must correspond to excitation into the 2^2B_g state, both states may contribute to the third PE band according to their Koopmans character (cf. "%K" in Table 1). Perhaps it is for this reason that the third PE band appears to be larger than the second one which is due to a state which carries only ≈50% Koopmans character according to INDO/S.

1,5-DHP$^{\bullet+}$. Finally, this tautomer has a *vinylbutadiene* π-chromophore which should express itself in yet another type of PE and EA spectrum with almost no precedent in the literature.[21] Some features of the electronic structure of this triene cation chromophore are quite similar to those of its linear conjugated tautomer (cf. INDO/S calculations): in both cases do we find a close-lying pair of low-lying excited configurations which arise from $\pi_2 \rightarrow \pi_3$ and $\pi_3 \rightarrow \pi_4^*$ electron promotion. However, if we assume "topological" C_{2v} symmetry for the vinylbutadiene π-system, these two configurations belong now to different representations and hence do not undergo the strong configuration interaction which is typical for linear conjugated polyene radical cations.[19] Instead, both are strongly stabilized through interaction with higher-lying NK configurations (see Figure 2c).

In this case we find again near perfect coincidence between the first EA and the second PE band, nonwithstanding the strong bond length changes between neutral and cation which are accompanied by a 0.3 eV relaxation energy (see section 3d). INDO/S calculations show that this is due to a fortuitious cancellation of effects as it is operative also in linear conjugated triene cations:[25] The first two excited configurations which are split by 1.3 eV at the neutral geometry become nearly degenerate in the cation, but nevertheless, the changes in the amount of CI with higher excited configurations are such that the final states undergo only slight shifts in energy upon relaxation of the cation

(14) (a) Zerner, M. C.; Ridley, J. E. *Theor. Chim. Acta* **1973**, *32*, 111; (b) Edwards, W. D.; Zerner, M. C. *Theor. Chim. Acta* **1987**, *72*, 347. (c) a) Zerner, M. C.; Quantum Theory Project, University of Florida, Gainesville; program available from the author upon request.

(15) Pople, J. A.; Beveridge, D. L.; Dobosh, P. A. *J. Chem. Phys.* **1967**, *47*, 2026. A multiplication factor of 540 G was used to convert hydrogen 1s spin populations to hyperfine couplings.

(16) Dewar, M. J. S.; Zoebisch, E. G.; Healy, E. F.; Stewart, J. J. P. *J. Am. Chem. Soc.* **1985**, *107*, 3902. Hydrogen 1s spin densities after annihilation were multiplied by 1177 G to obtain the hyperfine coupling constants (Clark, T.; Nelsen, S. F. *J. Am. Chem. Soc.* **1988**, *110*, 868).

(17) (a) Brogli, F.; Clark, P. A.; Heilbronner, E.; Neuenschwander, M. *Angew. Chem.* **1973**, *85*, 414. (b) Spectrum depicted in: Schafer, O. Ph.D. Thesis No. 1011, University of Fribourg, Switzerland, 1992.

(18) We had previously noted a similar absence of discernible visible absorptions in the radical cation of dimethylfulvene (Truttmann, L.; Bally, T. Unpublished work).

(19) For discussions of the electronic structure of linear conjugated polyene radical cations, see: (a) Bally, T.; Nitsche, S.; Roth, K.; Haselbach, E. *J. Am. Chem. Soc.* **1984**, *106*, 3927. (b) Bally, T.; Roth, K.; Tang, W.; Schrock, R. R.; Knoll, K.; Park, L. Y. *J. Am. Chem. Soc.* **1992**, *114*, 2440. (c) Fülscher, M.; Bally, T.; Matzinger, S. *Chem. Phys. Lett.* **1995**, *236*, 167.

(20) (a) By "non-Koopmans" we denote states which are dominated by configurations formed by excitation into virtual MOs, configurations whose energy can therefore not be directly related to MO energies according to Koopmans' theorem. (b) Due to the selection rules governing single-photon ionization such states do not contribute to the PE spectra (except if "Koopmans" configurations are admixed).

(21) Out of the more than 100 cross-conjugated polyenes ("dendralenes")[22] which have been described so far, only one has been studied by PE-spectroscopy,[23] in spite of the unabated interest in this class of hydrocarbons.[24]

(22) Hopf, H. *Angew. Chem., Int. Ed. Engl.* **1984**, *23*, 984.

(23) Bally, T.; Neuhaus, L.; Nitsche, S.; Haselbach, E.; Janssen, J.; Lüttke, W. *Helv. Chim. Acta* **1983**, *66*, 1288.

(24) See, for example: Trahanowsky, W. S.; Koeplinger, K. A. *J. Org. Chem.* **1992**, *57*, 4711.

(25) CASSCF/CASPT2 calculations on the first few members of the series of polyenes and their radical cations have shown that—by a fortuitious cancellation of effects—the energies of the first two excited states are virtually unaffected by the pronounced bond length changes which which occur upon relaxation of the radical cations.[19c]

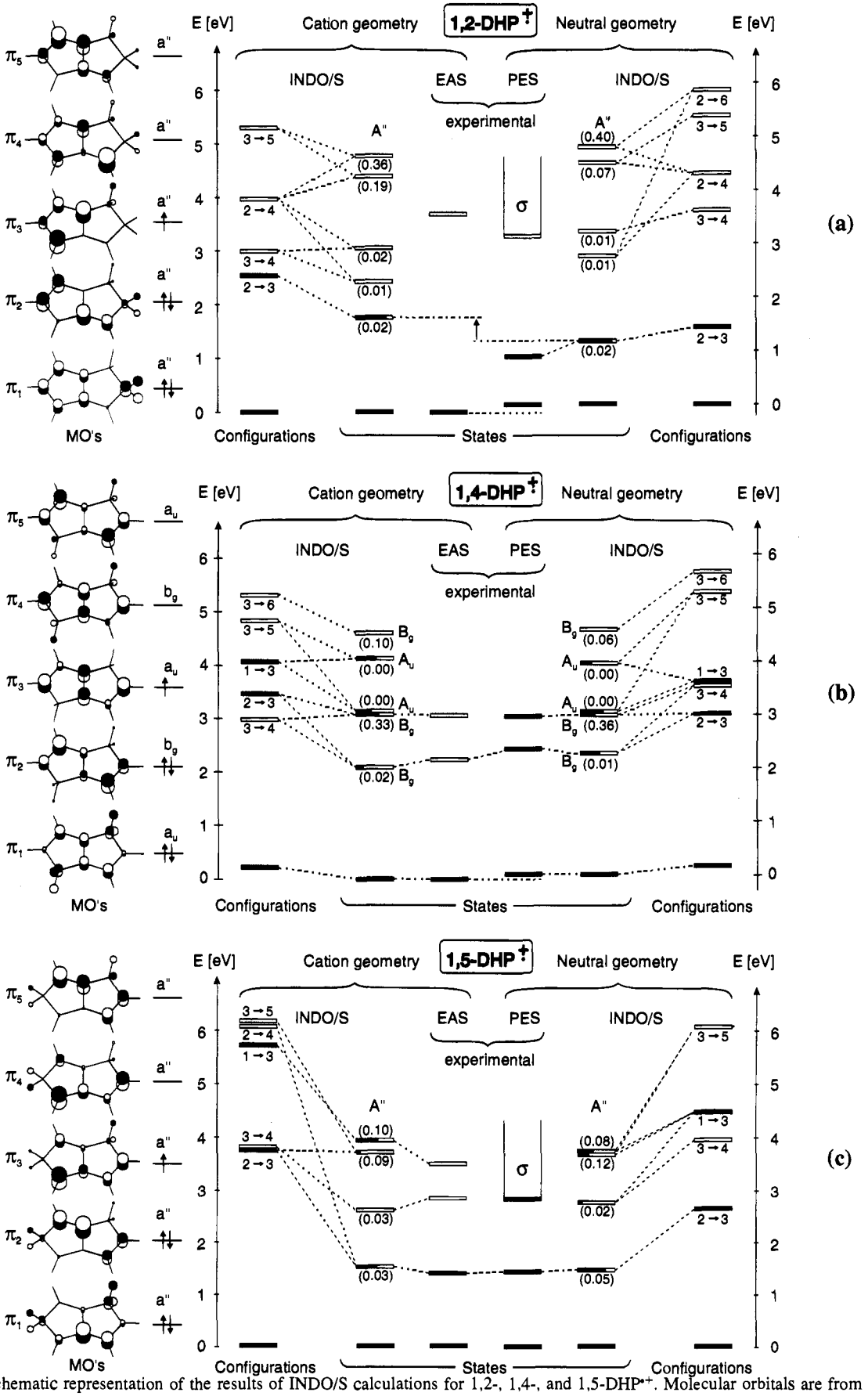

Figure 2. Schematic representation of the results of INDO/S calculations for 1,2-, 1,4-, and 1,5-DHP$^{\bullet+}$. Molecular orbitals are from RHF/3-21G calculations of the neutrals at the cation geometries. The outermost columns show the energies of one-electron configurations (solid bars: Koopmans, open bars: non-Koopmans configurations[20]); next to them are the energies of the final states which arise by mixing of these configurations (solid in proportion to Koopmans character[20]). In the two central columns the vertical excited state energies from the PE spectra (=neutral geometry) and the EA spectra (=cation geometry) are represented for comparison. Note that the ground state energies of 1,2- and 1,4-DHP$^{\bullet+}$ are displaced by the vibrational interval corresponding to $I_v - I_a$ in the PE spectra in order to make the excited state energies comparable.

Table 1. Ionic States of Dihydropentalenes (Compare Figure 2)[a]

			neutral geometry[b]					cation geometry[c]				
compd	state	symmetry	$I_{v,j}$ (PES)[d]	$-\epsilon_j$ (SCF)[e]	ΔE (PES)[f]	ΔE (INDO)[g]	% K (INDO)[h]	$-\epsilon_j$ (SCF)[e]	ΔE (EAS)[i]	ΔE (INDO)[g]	f (INDO)[i]	% K (INDO)[h]
1-2 DHP	$\tilde{X}$	$1^2A''$	**7.98**	7.97	(**0.00**)	(0.00)	98	7.12	(**0.00**)	(0.00)		98
	$\tilde{A}$	$2^2A''$	**8.95**	8.84	**0.97**	1.20	92	8.90	**?**	1.76	0.02	75
	$\tilde{B}$	$3^2A''$				2.77	<1		**?**	2.43	0.01	<1
	$\tilde{C}$	$4^2A''$				3.21	<1		**?**	3.05	0.02	<1
	$\tilde{D}$	$5^2A''$				4.50	<1		**3.70**	4.40	0.20	<1
	$\tilde{E}$	$6^2A''$		13.15		4.82	23	13.04		4.78	0.35	12
	(σ-st.)	$1^2A'$	**>11.10**	>12.63	**>3.12**	>4.26		>12.83		>5.07	<0.01	
1-4 DHP	$\tilde{X}$	1^2A_u	**7.48**	7.28	(**0.00**)	(0.00)	97	6.72	(**0.00**)	(0.00)		96
	$\tilde{A}$	1^2B_g	**9.89**	10.33	**2.41**	2.28	49	10.33	**2.26**	2.07	0.02	17
	$\tilde{B}$	2^2B_g				3.04	40		**3.08**	3.09	0.33	63
	$\tilde{C}$	2^2A_u	**10.41**	11.17	**2.93**	3.04	62	11.16		3.17	0.00	40
	$\tilde{D}$	3^2A_u				3.93	34			4.14	0.00	53
	(σ-st.)	$^2A_g/^2B_u$	**>11.40**	>13.03	**>3.92**	>4.77		>12.93		>5.14	<0.01	
1-5 DHP	$\tilde{X}$	$1^2A''$	**7.86**	7.73	(**0.00**)	(0.00)	98	7.19	(**0.00**)	(0.00)		98
	$\tilde{A}$	$2^2A''$	**9.29**	9.61	**1.43**	1.46	75	9.49	**1.43**	1.53	0.03	58
	$\tilde{B}$	$3^2A''$				2.79	15		**2.87**	2.61	0.03	<1
	$\tilde{C}$	$4^2A''$				3.69	15		**3.51**	3.72	0.09	14
	$\tilde{D}$	$5^2A''$		11.77		3.71	54	11.77		3.95	0.10	60
	(σ-st.)	$1^2A'$	**>10.72**	>12.32	**>2.86**	>3.86		>12.78		>4.43	<0.01	

[a] Experimental numbers are bold, calculated values normal. [b] For calculated values: fully optimized HF/6-31G* geometry. [c] For calculated values: fully optimized ROHF/6-31G* geometry. [d] Vertical ionization energies from PE spectra. [e] SCF MO-energy, 6-31G*. [f] Difference between jth and first vertical ionization energies. [g] INDO/S excited state energies. [h] Percent contribution of Koopmans configurations to final states. [i] Vertical excitation energies from electronic absorption spectra. [j] Oscillator strength for electronic transition.

Table 2. Comparison of Excited State Energies (in eV) of 1,4-DHP$^{\bullet+}$ and Hexatriene Radical Cation (HT$^{\bullet+}$) from experiment[19] and INDO/S Calculations

1,4-DHP$^{\bullet+}$		HT$^{\bullet+}$		difference	
exp	INDO/S	exp	INDO/S	exp	INDO/S
2.26	2.07	1.92	1.99	−0.34	−0.08
3.09	3.09	3.26	3.16	+0.17	+0.07

($\tilde{A}$: +0.07 eV; $\tilde{B}$: −0.18 eV; $\tilde{C}$: +0.03 eV), in accord with experimental observations.

The second, weakly structured EA band at ≈24 000 cm^{-1} can be attributed to the second (NK) excited state predicted at slightly lower energy by INDO/S. Its energetic proximity to the third PE band is accidental because the latter must be due to ionization from a σ-MO, as no π-states of appreciable Koopmans character are predicted to lie in this region. Finally, the intense band peaking at 28 300 cm^{-1} is probably due to the strongly allowed excitation into the highly mixed third and/or fourth excited state(s) which may also contribute to the PE cross section in this energy region.

(b) ESR Spectral Assignments of 1,2- 1,4-, and 1,5-DHP$^{\bullet+}$. A necessary prerequisite to the photochemical studies is the assignment of the ESR spectra initially obtained by the radiolytic oxidation of 1,2-, 1,4-, and 1,5-DHP. As discussed below, these spectra presented in Figures 3, 4a, and 5a are in close accord with expectations based on molecular orbital considerations and theoretical calculations for the respective radical cations of the parent compounds. Consequently, thermal rearrangement pathways do not appear to be accessible to this particular group of radical cations under the conditions used for their generation. Moreover, no evidence for thermal rearrangements was obtained over the range of matrix temperatures employed in these studies. As will be seen, these simplifying features greatly assist the interpretation of the photoinduced spectral changes starting from 1,4-DHP$^{\bullet+}$ and 1,5-DHP$^{\bullet+}$.

1,2-DHP$^{\bullet+}$. Figure 3 shows the ESR spectra (a), (b), and (c) obtained after the radiolytic oxidation of 1,2-DHP in three different Freon matrices. While the spectra are clearly quite similar in possessing an apparent quartet pattern with the same overall width (60 G), there is a gradual improvement in the resolution from (a) to (c), and the latter spectrum is well simulated in (d) using the hyperfine couplings given in Table 3. Essentially, the apparent quartet structure seen at low

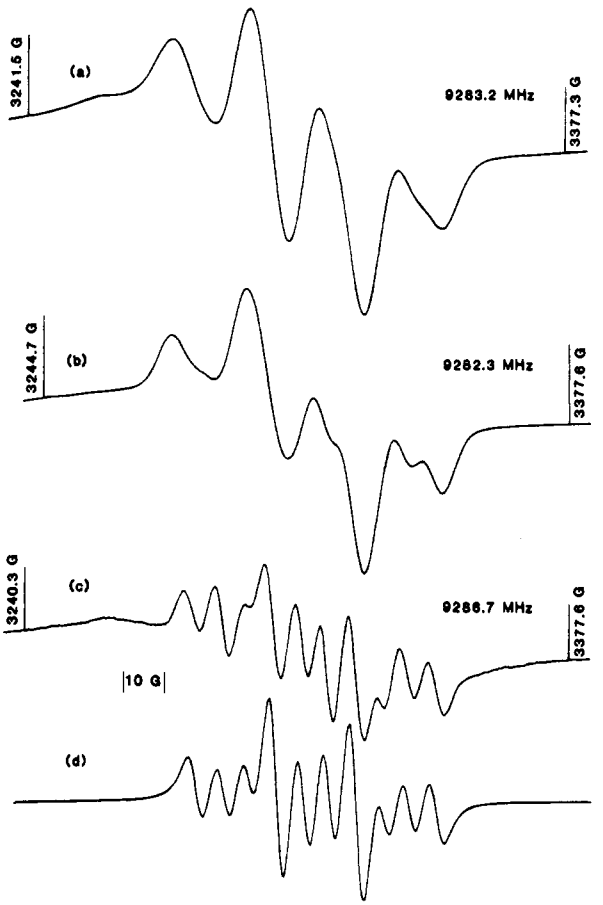

Figure 3. ESR spectra of 1,2-DHP$^{\bullet+}$ in $CFCl_2CFCl_2$ at 120 K (a), CF_2ClCCl_3 at 120 K (b), and $CF_2ClCFCl_2$ at 115 K (c). Spectrum d was simulated using the hyperfine parameters for 1,2-DHP$^{\bullet+}$ given in Table 3.

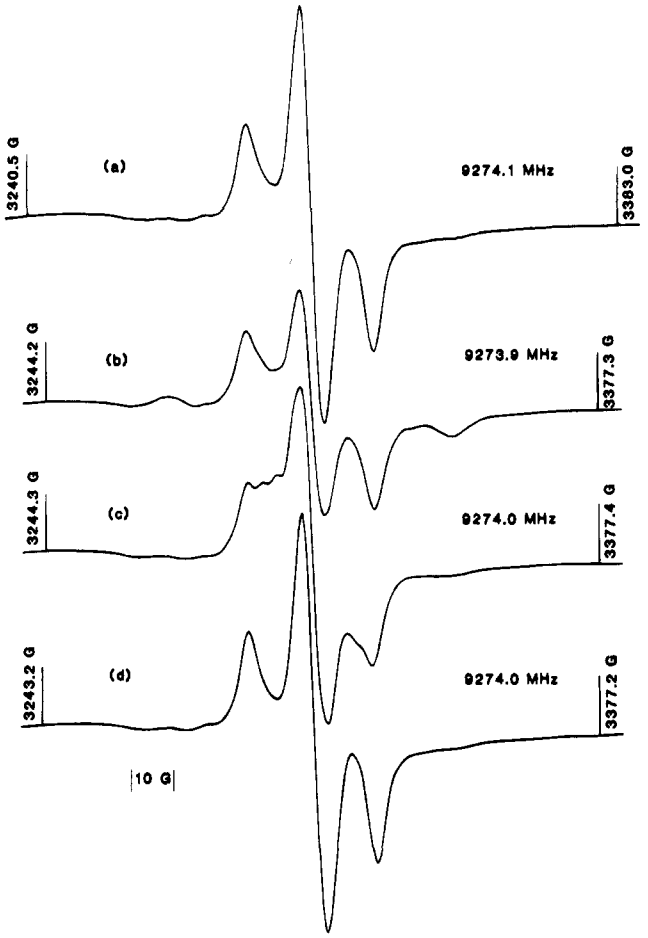

Figure 4. ESR spectra demonstrating a photochemical cycle in which the initially present 1,4-DHP$^{\bullet+}$ in CF_3CCl_3 at 120 K (spectrum a) was successively converted into 1,5-DHP$^{\bullet+}$ (λ = 408 nm, spectrum b) and 1,6-DHP$^{\bullet+}$ (λ > 840 nm spectrum c) and then quantitatively regenerated (λ > 640 nm, spectrum d). All spectra were recorded under exactly the same instrumental conditions. The same cycle was observed irrespective of whether the initial 1,4-DHP$^{\bullet+}$ was generated directly by radiolytic oxidation of the parent compound or by photochemical sequences starting from solid solutions of 1,5-DHP$^{\bullet+}$, 3a,6a-DHP$^{\bullet+}$, or the cyclooctatetraene radical cation (COT$^{\bullet+}$). For details of the instrumental conditions and filters used for the photolyses, see section 3b.

resolution results from the fact that the sum of the two unresolved doublet splittings (13.2 and 7.0 G) is equal to the 1:2:1 triplet splitting of 20.2 G. These doublet splittings are, however, quite well resolved in spectrum (c).

The assignment of this spectrum to 1,2-DHP$^{\bullet+}$ is straightforward on the basis of the agreement with AM1 and INDO calculations of the hyperfine splittings presented in Table 3. The 20.2 G triplet splitting is associated with the two equivalent hydrogens at the C-1 position, and the two doublet splittings are assigned to the hydrogens at C-4 and C-6, although the AM1 value for the latter is appreciably lower than the experimental result. The singly occupied MO (SOMO) for 1,2-DHP$^{\bullet+}$ shown as π_3 in Figure 2(a) is essentially concentrated in one ring on C-4, C-5, C-6, and C-6a with a perpendicular nodal plane passing through C-3a and bisecting this ring between C-5 and C-6. Since the largest MO coefficients are on C-4 and C-6a, the former gives rise to the strong α-hydrogen coupling at this position (H_4), while the latter results in large couplings to the two β-hydrogens at C-1. The remaining observed coupling is to the hydrogen at C-6, the MO coefficient at this position being larger than that at C-5, as shown in Figure 2(a).

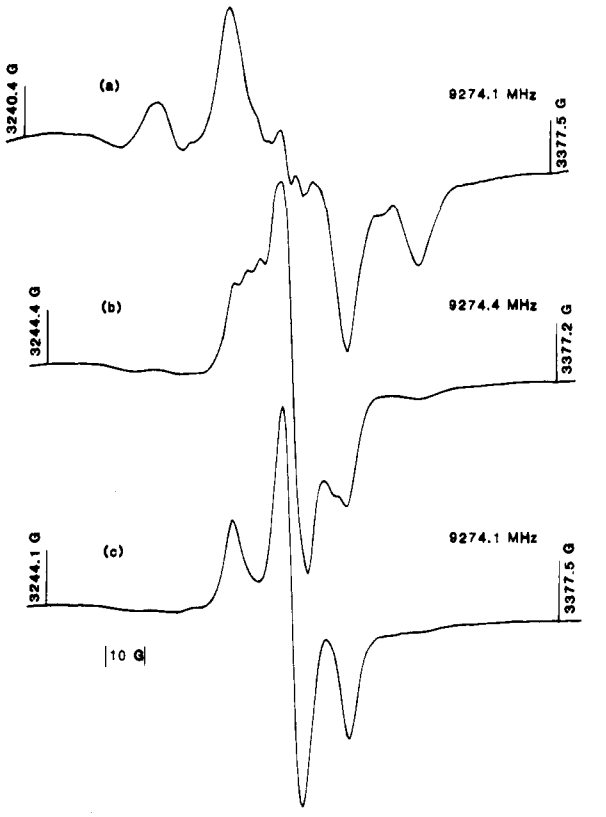

Figure 5. ESR spectra showing the consecutive photoconversion of the initially present 1,5-DHP$^{\bullet+}$ in CF_3CCl_3 at 120 K (spectrum a, after γ-irradiation of 1,5-DHP) into 1,6-DHP$^{\bullet+}$ (λ > 840 nm, spectrum b) and 1,4-DHP$^{\bullet+}$ (λ > 640 nm, spectrum c). Spectra a, b, and c here can be compared with the corresponding spectra b, c, and d in Figure 4, the spectral changes in each case resulting from the use of the same filtered light (see section 2(b) for details of filters, etc). All spectra were recorded under the same instrumental conditions (cf. Section 2b) except for relative gain settings of 1.0, 0.5, and 0.4 for spectra a, b, and c, respectively.

1,4-DHP$^{\bullet+}$. The ESR spectrum obtained after the radiolytic oxidation of 1,4-DHP in the CF_3CCl_3 matrix is shown in Figure 4(a) and consists of a well-defined 1:2:1 triplet structure in which the outer lines are broadened by hyperfine anisotropy. A virtually identical spectrum was similarly generated from 1,4-DHP in the CF_2BrCF_2Br matrix.[3] The form of the spectrum immediately suggests that the hyperfine splitting (11.9 G) results from interaction with two equivalent α-hydrogens. This result accords with the calculations for 1,4-DHP$^{\bullet+}$ (Table 3) showing that only the α-hydrogens at C-2 and C-5 are strongly coupled with predicted splittings close to 10 G. 1,4-DHP$^{\bullet+}$ belongs to the C_{2h} point group, and, as expected for the cation of a linear conjugated triene, the largest coefficients for the π_3 (a_u) SOMO in Figure 2(b) are located at these C-2 and C-5 symmetry-equivalent positions which form the termini of the π system.

This assignment of the 1,4-DHP$^{\bullet+}$ spectrum implies that the couplings to the remaining two sets of equivalent hydrogens are less than the line width (ca. 5 G). First, a small coupling to the α-hydrogens at C-3 and C-6 is understandable because of the small π spin densities at these positions. Secondly, the equivalent β-hydrogens at C-1 and C-4 are both subject to a strong cancellation effect resulting from the opposite signs of the SOMO coefficients at the adjacent carbons, these sign changes being evident from the plot of π_3 (a_u) in Figure 2(b). As pointed out originally by Whiffen,[26] it is the square of the algebraic sum of these coefficients that determines the β-hy-

(26) Whiffen, D. H. *Mol. Phys.* **1963**, *6*, 223.

Table 3. Experimental and Calculated ESR Parameters of Dihydropentalene (DHP) Radical Cations

radical cation	matrix	T (K)	g_{iso}	source of hf data	hyperfine couplings (G)
1,2-DHP$^{\bullet+}$	$CF_2ClCFCl_2$	115	2.0026	expt[a]	20.2(2H), 13.2(1H), 7.0(1H)
				AM1[b]	18.8($2H_1$), −11.3($1H_4$), −2.6($1H_6$)
				INDO[c]	22.1($2H_1$), −12.5($1H_4$), −4.1($1H_6$)
1,4-DHP$^{\bullet+}$	CF_3CCl_3	120	2.0029	expt[a]	11.9(2H)
				AM1[b]	-10.3(H_2 and H_5),[d] 4.4(H_3 and H_6),[d] 2.4($2H_1$ and $2H_4$)[d]
				INDO[c]	−7.8(H_2 and H_5),[d] 1.5(H_3 and H_6),[d] 2.1($2H_1$ and $2H_4$)[d]
1,5-DHP$^{\bullet+}$	CF_3CCl_3	120	2.0033	expt[a]	20.0(2H), 14.3(1H), 5.6(2H)
				AM1[b]	15.9($2H_1$), −12.7($1H_4$), 9.4($2H_5$), −6.3($1H_2$), −6.2($1H_6$)
				INDO[c]	19.6($2H_1$). −12.1($1H_4$). 9.7($2H_5$), −3.3($1H_2$), −5.4($1H_6$)
1,6-DHP$^{\bullet+}$	CF_3CCl_3	120	2.0028	expt[a]	*ca.* 10.0(2H), *ca.* 3.5(2H)
				AM1[b]	8.6 ($2H_1$ and $2H_6$),[d] −8.2(H_2 and H_5),[d] 4.4(H_3 and H_4)[d]
				INDO[c]	7.9 ($2H_1$ and $2H_6$),[d] −5.8(H_2 and H_5),[d] 1.0(H_3 and H_4)[d]
3a,6a-DHP$^{\bullet+}$	$CF_2ClCFCl_2$	108	2.0029	expt[a]	36.2(2H), 7.7(4H)
				AM1[b]	30.9(H_{3a} and H_{6a}),[e] −8.0(H_1 and H_3 and H_4 and H_6),[d] 5.6(H_2 and H_5)[d]
				INDO[c]	44.2(H_{3a} and H_{6a}),[e] −6.6(H_1 and H_3 and H_4 and H_6),[d] 3.6(H_2 and H_5)[d]

[a] This work. [b] Reference 16. AM1 optimized geometries. [c] Reference 15; ROHF/6-31G* optimized geometries. [d] Hydrogens at different ring positions rendered equivalent by symmetry. [e] Bridgehead hydrogen atoms.

drogen coupling in this case. Consequently, even a minor spin population on one of the carbons brings about a disproportionately large effect on the coupling anticipated from the other site of major spin density.[27] For example if the spin populations on the adjacent carbons are 4ϱ and 1ϱ, then the coupling to the β-hydrogens of the bridging methylene group is proportional to 9ϱ for coefficients of like sign but only to 1ϱ for coefficients of opposite sign. Accordingly, the absence of resolvable couplings to the β-hydrogens at C-1 and C-4 of 1,4-DHP$^{\bullet+}$ can be attributed to the opposite signs of the SOMO coefficients at the adjacent carbons of these bridging methylene groups.

1,5-DHP$^{\bullet+}$. Figure 5(a) shows the ESR spectrum recorded after the radiolytic oxidation of 1,5-DHP in CF_3CCl_3. Although the first-derivative spectrum is not fully resolved, there are four broad components with the low-field and high-field pairs showing strong positive and negative excursions, respectively, above the baseline. These prominent features were simulated by means of the coupling constants reported in Table 3 which are in satisfactory agreement with the calculated values except for the absence of the predicted 9 G couplings to the two equivalent hydrogens at C-5. It is to be noted, however, that the couplings to these β-hydrogens are subject to the cancellation effect (vide supra) resulting from the presence of opposite SOMO coefficients at the adjacent C-4 and C-6 carbons, as can be seen from the representation of π_3 in Figure 2(c). It is quite likely, therefore, that the coupling to these β-hydrogens at C-5 is overestimated by the calculations.

The largest 2H coupling of 20 G is assigned to the two β-hydrogens at C-1. Here it is significant that the SOMO coefficients at C-2 and C-6a have the same sign in contrast to the case just discussed for the β-hydrogens at C-5. The importance of the sign relationship can also be adduced from the fact that the β-hydrogen couplings at C-1 are larger than at C-5 although the SOMO coefficients at the adjacent carbons are distinctly smaller in the former case (Figure 2(c)). The remaining couplings are assigned to the α-hydrogens at C-4, C-6, and C-2 since these represent the major sites of spin populations. The SOMO representation in Figure 2(c) as well as the calculations clearly indicate that the largest spin density resides on C-4, and therefore the coupling of 14.3 G is assigned to H_4. The other two hydrogens at C-6 and C-2 are both estimated to have couplings of ca. 5.6 G, in good agreement with the results of the AM1 calculations (Table 3).

(c) Photochemistry in Freon Glasses. The photochemical formation of 1,4- from 3a,6a-DHP$^{\bullet+}$ was described previously.[3] After realizing that H-shifts can be induced photochemically in DHP$^{\bullet+}$ we engaged in a search for further rearrangements of this kind, a search which found abundant reward, as shown below.

Thus, irradiation of 1,4-DHP$^{\bullet+}$ at 400 nm resulted in its complete conversion to new species as shown in Figure 6a,b. One of these photoproducts can be readily identified as 1,5-DHP$^{\bullet+}$ on the basis of the authentic spectrum, reproduced for reference purpose in Figure 6c. Subsequent irradiation at 800 nm bleached 1,5-DHP$^{\bullet+}$ with concomitant enrichment of the other photoproduct which had already been formed in the photolysis of 1,4-DHP$^{\bullet+}$. The general habitus of the EA spectrum of this species (Figure 6d) is very similar to that of 1,5-DHP$^{\bullet+}$ which suggests a similarity of the π-chromophore. For comparison we show the spectrum of 2-vinyl-1,3-cyclohexadiene radical cation[28] (another hydrocarbon with a vinylbutadiene π-system) whose first band happens to be almost superimposable to that of the above photoproduct (Figure 6d/e). Since there is only one additional DHP$^{\bullet+}$ tautomer which possesses a π-system of vinylbutadiene topology (cf. Scheme 1), we believe that the new species observed in the above photolyses is identifiable as 1,6-DHP$^{\bullet+}$.

Confirmation of this consecutive photochemical reaction sequence from 1,4-DHP$^{\bullet+}$ to 1,6-DHP$^{\bullet+}$ through the intermediacy of 1,5-DHP$^{\bullet+}$ is provided by the ESR results shown in Figures 4 and 5. First, the spectral change 4a → 4b on irradiation of 1,4-DHP$^{\bullet+}$ clearly results in the growth of additional features in the wings which correspond to the broad outer lines of the 1,5-DHP$^{\bullet+}$ spectrum in Figure 5a. It is also noteworthy that, relative to the intensity of the center line, the pair of inner features flanking this line is both broader and more intense in spectrum 3b than is the case for the initial spectrum 4a of 1,4-DHP$^{\bullet+}$, indicating that these features are not mainly attributable to unreacted 1,4-DHP$^{\bullet+}$. In fact, these flanking inner features can also be assigned to 1,5-DHP$^{\bullet+}$ by comparison with spectrum 5a. While we cannot rule out that some minor residual 1,4-DHP$^{\bullet+}$ contributes to the three center components of 4b, it is likely that the latter spectrum is mainly composed of 1,5-DHP$^{\bullet+}$ and 1,6-DHP$^{\bullet+}$ in complete parallel with the results obtained by EA spectroscopy (vide supra). Thus, the center line in 4b which cannot be assigned to 1,5-DHP$^{\bullet+}$ is consistent with its spectral assignment to 1,6-DHP$^{\bullet+}$, as described below.

The ESR studies also provide independent evidence for the $\lambda > 840$ nm photobleaching of 1,5-DHP$^{\bullet+}$ to 1,6-DHP$^{\bullet+}$ in the

(27) Williams, F. J. *Phys. Chem.* **1994**, *98*, 8258

(28) Bally, T.; Roth, K.; Pürro, P. unpublished (reproduced from: Roth, K., Ph.D. Thesis No. 958, University of Fribourg, 1989).

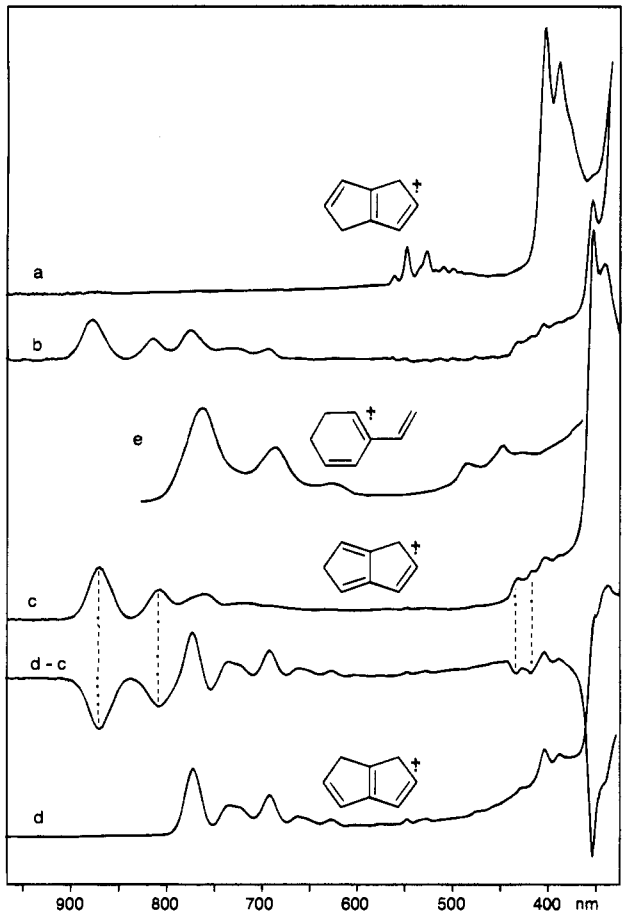

Figure 6. EA spectrum of ionized 1,4-DHP before (a) and after narrow-bandwidth irradiation at ≈400 nm (b). Same for ionized 1,5-DHP before (c) and after irradiation at $\lambda > 800$ nm (d). Spectrum (d-c) is the difference spectrum which shows the decreasing bands of 1,5-DHP$^{\bullet+}$ (cf. dashed lines) and the increasing bands of the photoproducts 1,4-DHP$^{\bullet+}$ (550–500 and ≈400 nm) and 1,6-DHP$^{\bullet+}$ (800–600 nm). Spectrum (e) is the spectrum of ionized 2-vinyl-1,3-cyclohexadiene.[28]

second step, as revealed by the spectral changes 4b → 4c and 5a → 5b. In each case there is a narrowing of the spectrum and the resulting pattern is analyzed as a 1:2:1 triplet (a(2H) = 10 G) with a poorly resolved triplet substructure (a(2H) ca. 3.5 G). At first sight, these parameters do not seem to be in accord with the calculated hyperfine splittings for 1,6-DHP$^{\bullet+}$ given in Table 3. However, the predicted splittings in the range of 7.6–9.2 G for the four equivalent β-hydrogens at C-1 and C-6 are thought to be of questionable accuracy since these couplings are again strongly influenced by the cancellation effect similar to that already described for 1,4- and 1,5-DHP$^{\bullet+}$. In the present case, the SOMO coefficients at the symmetry-equivalent C-2 and C-5 positions are of opposite sign to the smaller coefficient at C-6a, leading to a "negative" Whiffen effect[3,26,27] for the hydrogens of the bridging methylene groups at C-1 and C-6. Accordingly, if we assume that these β-hydrogen couplings are in fact negligible, then there is reasonable agreement with the calculations, and the triplet splittings of 10 and ca. 3.5 G can be readily assigned to H_2, H_5, and H_3, H_4, respectively, these couplings to α-hydrogens reflecting the spin distribution at the corresponding carbons of the π system.

Both EA and ESR results show that in contrast to 1,5-DHP$^{\bullet+}$, the 1,6-tautomer is quite insensitive to irradiation at the wavelength of its first absorption band, but upon decrease of the irradiation wavelength to $\lambda = 450$ nm in the EA studies, efficient photochemical conversion back to 1,4-DHP$^{\bullet+}$ sets in (see Figure 7), thus indicating the presence of an additional

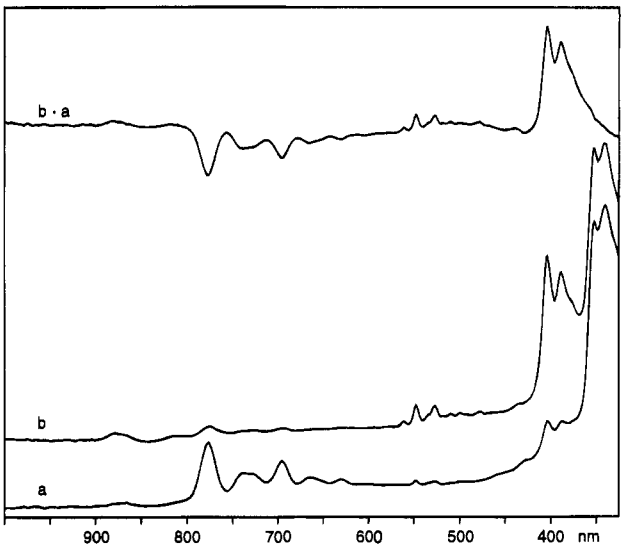

Figure 7. EA spectrum of 1,6-DHP$^{\bullet+}$ (formed photochemically from 1,5-DHP$^{\bullet+}$, cf. Figure 6d) before (a) and after irradiation at 450 nm (b). Note that the intensities of spectra 6a and 7b are nearly identical which indicates full recovery of 1,4-DHP$^{\bullet+}$ in the photochemical cycle.

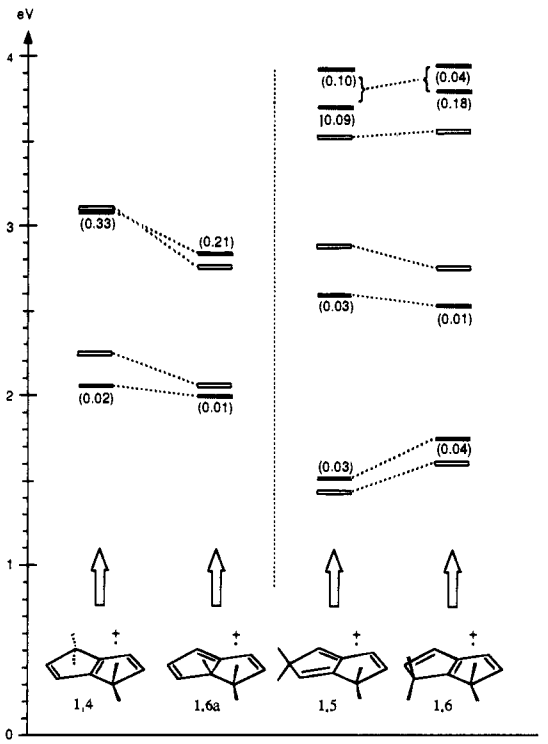

Figure 8. Results of INDO/S calculations for 1,4- and 1,6a-DHP$^{\bullet+}$ (=linear conjugated triene cations) as well as for 1,5- and 1,6-DHP$^{\bullet+}$ (=2-vinylbutadiene cations). Solid bars are from calculations (oscillator strengths in parentheses); open bars are observed excited state energies (indirectly in the case of the first excited state of 1,6a-DHP$^{\bullet+}$, see text).

excited state of 1,6-DHP$^{\bullet+}$ in this region. There is a weak feature at 470 nm in spectrum 6d which could correspond to the state observed at ≈420 nm in 1,5-DHP$^{\bullet+}$ (cf. dashed lines). According to INDO/S this state is indeed shifted to slightly lower energies (Figure 8), while at the same time the oscillator strength for the electronic transitions drops to one-third of the value in 1,5-DHP$^{\bullet+}$. Both predictions are in agreement with our observations, although the energy of this second excited state is ≈0.5 eV too low by INDO/S. The ESR studies also reveal a very clean quantitative conversion of the 1,6-DHP$^{\bullet+}$ back to 1,4-DHP$^{\bullet+}$, as shown in Figures 4c → 4d and 5b → 5c.

In this case the photobleaching was efficient even at 640 nm. However, this region of irradiation is still on the short-wavelength side of the main 1,6-DHP$^{\bullet+}$ absorption bands located at 700−800 nm (Figure 6).

In this way the photochemical cycle which had started with the irradiation of 1,4-DHP$^{\bullet+}$ is closed. Actually, this cycle can be followed several times with only small losses of intensity in the EA or ESR spectra. However, photolysis through Pyrex (>320 nm) at any stage of the photochemical cycle leads to irreversible bleaching of all DHP$^{\bullet+}$ isomers absorbing at >350 nm and to formation of a new product whose main absorption is at 340 nm and which shows no palpable features in the visible or NIR region. We can only speculate about the identity of the "photochemical sink". Although similar, its EA spectrum is distinct from that of 1,2-DHP$^{\bullet+}$ (which is also entirely photostable to visible irradiation), and most probably it also does not correspond to any of the remaining DHP$^{\bullet+}$ tautomers.[29] This leaves the possibility of a ring-opened product such as 1- or 6-vinylfulvene radical cation which would be in accord with the similarity to 1,2-DHP$^{\bullet+}$ which also has a fulvene chromophore and lacks prominent visible bands.

(d) Photochemistry in Argon Matrices: The Missing Link. Scheme 1 suggests that the formation of 1,4- from 3a,6a-DHP$^{\bullet+}$ involves 1,3a- or 1,6a-DHP$^{\bullet+}$ as a "stepping stone" and that this species would remain accessible by single H-shifts from all the other observed DHP$^{\bullet+}$ tautomers. Thus, the photochemical cycle presented above contains a missing link which we believe to have discovered from EA studies by modifying the conditions of our experiments, in particular by changing the medium to argon matrices.

By and large, the photochemical processes observed in these experiments take the same course as those described above in Freon glasses, i.e., conversion of 3a,6a-DHP$^{\bullet+}$ to 1,4-DHP$^{\bullet+}$ is induced by irradiation of the former at λ > 630 nm (see Figure 9a,b). However, a new species with a sharp band at 450 nm is now observed which disappears together with 1,4-DHP$^{\bullet+}$ upon irradiation at λ = 400 nm (Figure 9c). If the mixture of 1,5- and 1,6-DHP$^{\bullet+}$ obained in this way (or ionized 1,5-DHP$^{\bullet+}$) is bleached persistently through a 630 nm cutoff filter, the 450 nm band arises quite prominently next to the bands of 1,4-DHP$^{\bullet+}$ with a weak, broad feature at 540−630 nm.[31] Subsequent photolysis at λ > 540 nm (Figure 9d) leads to the concerted disappearance of both this broad feature and the sharp 450 nm band (cf. difference spectrum, Figure 9e) thus indicating that they belong to the same species, while at the same time 1,4-DHP$^{\bullet+}$ is re-formed quantitatively.

Notwithstanding the difference in shape of the first band, the general habitus of this new spectrum (weak low energy, intense high-energy band) is similar to that of 1,4-DHP$^{\bullet+}$ which suggests

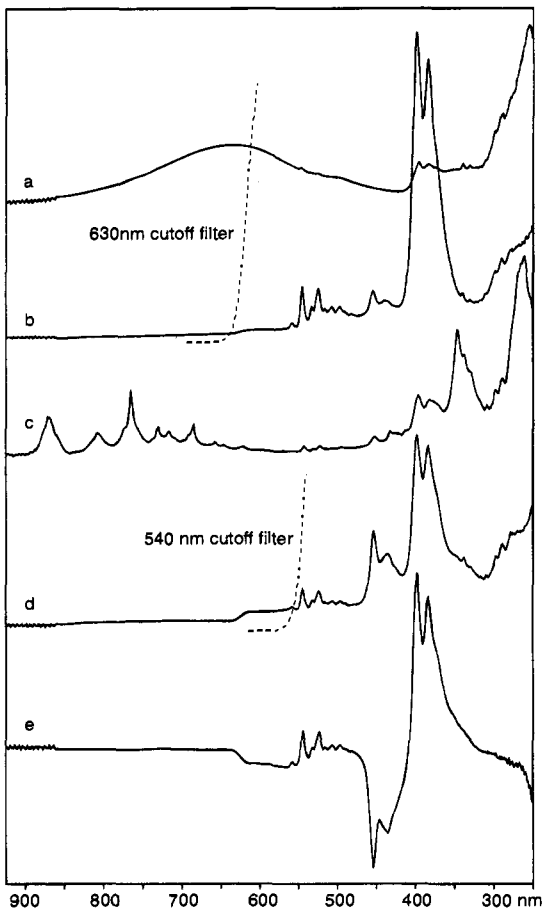

Figure 9. (a) Spectrum of 3a,6a-DHP$^{\bullet+}$ (obtained from ionized COT) in an argon matrix before (a) and after photolysis at >630 nm (b). Spectrum (c) is obtained upon irradiation at ≈400 nm (comparison with spectrum 6b shows that the bands of 1,5- and 1,6-DHP$^{\bullet+}$ are sharper in argon matrices). Subsequent photolysis at >630 nm leads to spectrum (d) which can be transformed back cleanly to 1,4-DHP$^{\bullet+}$ (cf. Figure 6a) by irradiation through a 540 nm cutoff filter (see difference spectrum e).

that it could be due to another species with a linear conjugated triene chromophore. There is only one such compound left in our scheme of DHP$^{\bullet+}$ tautomers (Scheme 1), namely 1,6a-DHP$^{\bullet+}$, which can also be formed from any of the other isomers observed in this study by a single H-shift. Indeed, INDO/S predicts a pronounced red-shift of the strong second absorption band between 1,4- and the related 1,6a-DHP$^{\bullet+}$, whereas the weak first band is only slightly displaced (see Figure 8). Both features are in agreement with the above assignment. However, since we will argue below that 1,6a-DHP$^{\bullet+}$ undergoes efficient *thermal* conversion to the 1,4-tautomer upon formation from 3a,6a-DHP$^{\bullet+}$, the present assignment would require that this conversion is ineffective when 1,6a-DHP$^{\bullet+}$ is formed from the 1,5- (or the 1,6-) tautomer. We will discuss this intriguing (but not unrealistic) possibility in the section on the orbital symmetry rules for DHP$^{\bullet+}$ interconversions.

Thus it appears that we have been able to identify six of the ten possible DHP$^{\bullet+}$ tautomers either by independent synthesis (four in this way, if one includes semibullvalene as a precursor to 3a,6a-DHP$^{\bullet+}$) and/or photochemical formation (1,6- and 1,6a-DHP$^{\bullet+}$). The remaining four isomers (1,3-, 1,3a-, 2,3a-, and 2,5-DHP$^{\bullet+}$) are much higher in energy (see following section), and their electronic structures are incompatible with any of the EA spectra observed in the present experiments.[29]

(e) Thermochemistry of DHP$^{\bullet+}$ Tautomers. In order to assess the relative stability of the DHP$^{\bullet+}$ tautomers (which will

(29) The 1,3-, 1,3a-, and 2,3a-isomers are expected to show broad weak charge-transfer bands next to the absorptions typical of the cyclopentadienyl[30a] (1,3) or pentadienyl cation[30b] (2,3a) or cyclopentadiene$^{\bullet+}$ [30c] (1,3a), while the spectrum of the 2,5 isomer will probably look similar to that of the other bisallylic isomer, 3a,6a-DHP$^{\bullet+}$, i.e., show a broad charge resonance band in the visible or NIR spectral region.

(30) (a) The cyclopentadienyl cation has never been observed by optical spectroscopy. Recent CI calculations for the most stable singlet predict weak transtions at 1000 and 247 nm and a strong one at 395 nm (Feng, J.; Leszczynski, J.; Weimer, B.; Zerner, M. *J. Am. Chem. Soc.* **1989**, *111*, 4648). (b) 1,1,5,5-Tetramethylpentadienyl cation has λ_{max} = 391 nm (Sorensen, T. S. *J. Am. Chem. Soc.* **1965**, *87*, 5075; the parent compound has never been observed). (c) Cyclopentadiene radical cation has a structured broad band system at 555 nm plus a sharp peak at 368 nm (Shida. T. *Electronic Absorption Spectra of Radical Ions*; Elsevier: Amsterdam, 1988).

(31) Upon repeating the same experiment in Freon glasses, where the photolysis of 1,6-DHP$^{\bullet+}$ is quite inefficient, we found that the 450 nm band arises also under these conditions but never gains the prominence it attains in argon matrices. It is also interesting to note that a similar peak is already discernible in the spectra of Shida et al. (Figure 16 in ref 1).

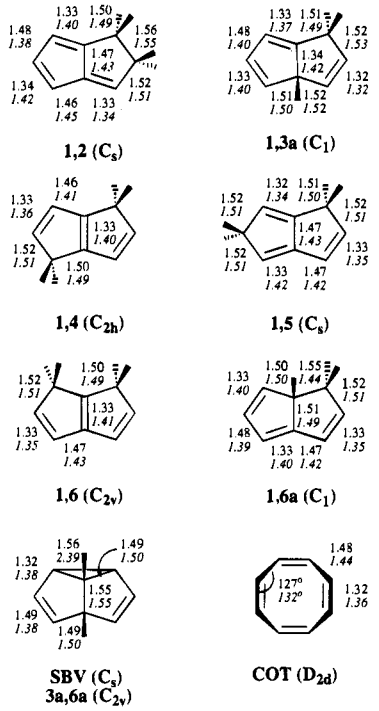

Figure 10. Bond lengths in neutral (regular type) and ionic (italic type) dihydropentalene tautomers from full SCF (radical cations: ROHF) geometry optimizations with the 6-31G* basis set. Resulting symmetries in parentheses. Note that semibullvalene (SBV) relaxes to the symmetric 3a,6a-DHP$^{\bullet+}$ upon ionization.

Table 4. Relative Energies (in kcal/mol) of Dihydropentalene (DHP) Tautomers and Their Radical Cations and Some Related C_8H_8 Valence Isomers, Completely Optimized at the SCF (ROHF) Level with the 6-31G* Basis set (see Figure 10 and Scheme 1 for Structures)

DHP tautomer[a]	neutral		radical cation		relaxation energy[b]
	SCF	MP2	ROHF	RMP2	
1,2	(0.00)[c]	(0.00)[d]	(0.00)[e]	(0.00)[f]	9.46
1,4	3.58	1.68	−2.61	−7.64	6.00
1,5	1.23	1.71	1.25	4.06	6.92
1,6	4.44	2.82	0.25	1.64	6.14
1,6a	7.53	6.04	6.10	2.22	7.91
1,3a	10.87	10.06	18.23	17.00	7.75
3a,6a	22.38[g]	14.97[g]	21.82	6.18	38.47[g]
2,3a	*h*	*h*	30.74	36.05	*h*
2,5	*h*	*h*	44.75	*i*	*h*
COT	14.68	22.55	26.25	19.56	14.46
1-VF[k]	12.71	17.56	13.14	13.63	
6-VF[l]	9.35	14.51	12.62	*i*	

[a] All geometries fully optimized at thge ROHF/6-31G* level; see Scheme 1 for the structures of the most important isomers. [b] Energy gained by relaxation of the cation from the neutral geometry, evaluated at the ROHF level. [c] Total energy: −307.544 762 au. [d] Total energy: −308.559 160 au. [e] Total energy: −307.317 127 au. [f] Total energy: −308.303 774 au. [g] Neutral geometry: semibullvalene. [h] No stable neutral structure. [i] No convergence achieved. [k] 1-Vinylfulvene (valence isomer and thermal precursor of 1,2-DHP[5]). [l] 6-Vinylfulvene (valence isomer of 1,6a-DHP).

be needed in the ensuing discussion of their interconversions in terms of orbital symmetry rules) we resorted to ab initio calculations at a level accounting for correlation effects. In our preceding papers,[3,4] we had already reported QCISD-calculations on the symmetric 3a-6a- and 1,4-DHP$^{\bullet+}$. This level of theory, although certainly very reliable, proved too costly for a systematic study of the $C_8H_8^{\bullet+}$ potential energy surface involving also the less symmetric tautomers. Since recent experience[32] has made us skeptical toward the results of many-body

(32) Bally, T.; Jungwirth, P. *J. Am. Chem. Soc.* **1993**, *115*, 5776, 5783.

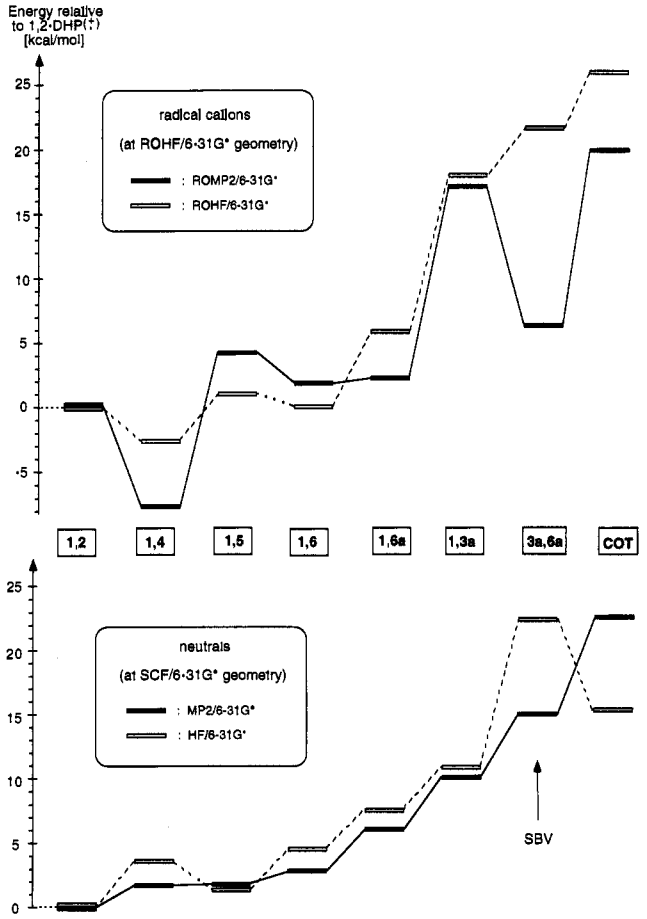

Figure 11. Relative energies (cf. Table 4) of neutral and ionic dihydropentalene tautomers from (RO)HF/6-31G* (open bars) and (RO)MP2/6-31G* calculations (solid bars) at the (RO)HF/6-31G* optimized geometries shown in Figure 8. The entries for neutral 3a,6a-DHP represent semibullvalene (SBV).

perturbation theory (MPBT) calculations based on UHF wave functions (such as UMP2),[33] we resorted to the recently developed programs permitting ROHF-based MBPT calculations[12] for reference purposes. Table 4 lists the relative energies of all ten DHP$^{\bullet+}$ and those of some related C_8H_8 isomers as obtained by single point MBPT2 calculations at the ROHF/6-31G* optimized geometries shown partly in Figure 10. For those tautomers possessing stable neutral closed-shell counterparts, the corresponding numbers were also calculated. The results are graphically represented in Figure 11.

Notable features of these results are the following:

(a) In the neutrals, the most stable tautomer is calculated to be 1,2-DHP, in agreement with experiment,[5] while, in the radical cations, 1,4-DHP$^{\bullet+}$ is clearly the most stable species.

(b) Correlation effects (as expressed by the difference in relative energy between the open and filled bars in Figure 11) play an important role in shaping the potential energy surface comprising the species discussed in the present work. In the neutrals, the most notable effect is the reversal of stabilities between COT and SBV.[34] In the radical cations, 3a,6a-DHP$^{\bullet+}$

(33) See, for example: Nobes, R. H.; Pople, J. A.; Radom, L.; Handy, N. C.; Knowles, P. *J. Chem. Phys. Lett.* **1987**, *138*, 481.

(34) This result is surprising in view of the experimentally determined *endo*thermicity of the COT → SBV reaction ($\Delta H° = 2.37 \pm 0.11$ kcal/mol. Martin, H.-D.; Urbanek, T.; Walsh, R. *J. Am. Chem. Soc.* **1985**, *107*, 5332). While this number is overestimated considerably at the SCF level ($\Delta H° = 7.7$ kcal/mol), the MP2 model puts SBV at a thermochemical advantage over COT ($\Delta H° = -7.6$ kcal/mol). We have no explanation for this discrepancy between experiment and theory which is only rectified at the MP4 level (Truttmann, L. Unpublished results).

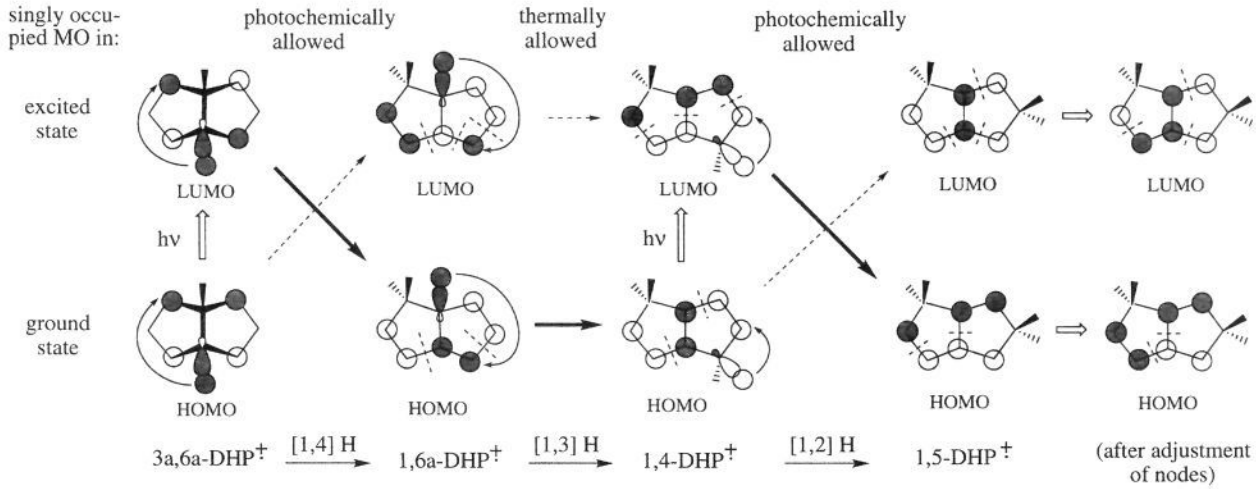

Figure 12. MO-correlation diagram for a selected series of H-shifts in DHP$^{\bullet+}$ tautomers (for discussion see text).

profits most strongly from stabilization through dynamic correlation which brings it into the same range of stabilities as 1,2-, 1,5-, 1,6-, and 1,6a-DHP$^{\bullet+}$. Somewhat smaller effects are found for 1,4- and 1,6a-DHP$^{\bullet+}$ as well as for COT$^{\bullet+}$.

(c) The first three photochemical reactions (COT$^{\bullet+}$ → 3a,6a-DHP$^{\bullet+}$ → 1,4-DHP$^{\bullet+}$) involve a ladder of exothermic processes, while the formation of 1,6- and 1,5-DHP$^{\bullet+}$ from 1,4-DHP$^{\bullet+}$ is endothermic. Importantly, the formation of 1,6a- from 1,6-DHP$^{\bullet+}$ is nearly thermoneutral, while it is predicted to be exothermic by ≈4 kcal/mol when originating from 3a,6a-DHP$^{\bullet+}$.

(f) Symmetry Control of H-Shifts in DHP$^{\bullet+}$. In view of the apparent selectivity of the various hydrogen shifts observed in this study, the question poses itself as to whether there might be rules which govern such rearrangements. We propose an FMO procedure which focuses on the nodal properties of the SOMOs in the reactant and product. The existence of a correlation between these two SOMOs determines in most cases whether a given H-shift is allowed thermally or photochemically (vide infra).

In terms of a specific prescription, the analysis proceeds by partitioning the reactant π-SOMO (HOMO for the ground state) into an empty p orbital, chosen so as to correspond to the position to which the hydrogen migrates, and the remnant SOMO. The migrating hydrogen is then transferred formally as a hydride ion to this empty p orbital thereby releasing a new p orbital at the original hydrogen site. This p orbital then combines with the remnant SOMO to form a new SOMO. Clearly, identical phases of the p orbitals at these sites of the dihydropentalene ring system must be maintained for suprafacial transfer.

Depending on the number of nodes in the emergent π-SOMO obtained in this way, one can see whether the radical cation product is formed in its ground state (SOMO = HOMO) or in an excited state (SOMO = LUMO or HOMO-1) and thus determine whether the reaction is thermally allowed or forbidden, respectively. Similarly, a reaction is photochemically allowed if the reactant LUMO or HOMO-1 correlates with the product HOMO (or if the SOMO corresponds to a low lying excited state of the product). If ambiguities with regard to the AO-signs at certain π-centers remain (for example because the corresponding coefficient was zero in the starting molecule), these are chosen such as to minimize the number of nodes in the product MO.

We wish to illustrate these rules (and possible problems in their application) by the sequence of reactions 3a,6a → 1,6a → 1,4 → 1,5-DHP$^{\bullet+}$ which we believe to have observed in the present study. Firstly, Figure 12 shows that the LUMO of 3a,6a-DHP$^{\bullet+}$ correlates with the HOMO of the 1,6a species, which in turn correlates with the HOMO of the 1,4 tautomer. Thus, we can formulate the photochemical conversion of 3a,6a- to 1,4-DHP$^{\bullet+}$ as proceeding via consecutive photoexcitation and thermal processes through the 1,6a intermediate (the exothermicity of the thermal conversion of 1,6a- to 1,4-DHP$^{\bullet+}$ is discussed further below).

Not unexpectedly, the predictions of these symmetry rules for open-shell radical cations can and do differ significantly from those of Woodward and Hoffmann which are applicable to closed-shell molecules.[35] For example, the thermally allowed conversion of 1,6a-DHP$^{\bullet+}$ to 1,4-DHP$^{\bullet+}$ in Figure 12 represents a suprafacial 1,3 hydrogen shift that would be Woodward–Hoffmann forbidden were the hole to be localized in either of the two double bonds *that do not shift* (which is, of course, quite unrealistic). Also, the general ease of 1,3 hydrogen shifts in radical cations has previously been pointed out by Clark[36] who carried out corresponding ab initio calculations on the propene radical cation. In particular, he showed that the transition state for the 1,3 hydrogen shift in this radical cation is suprafacial[36] in contrast to the high-energy antarafacial transition state for the neutral propene molecule.[35,37] The present work, therefore, accords with a substantial body of experimental and theoretical results[36,38,39] in suggesting that certain sigmatropic hydrogen shifts are much more facile in radical cations than in the corresponding parent molecules. Moreover, the symmetry rules developed here offer a simple codification that goes well beyond the prediction of 1,3 shifts. Clearly, these rules should be subjected to further tests as the chemistry of organic radical cations is systematically explored.

Other applications of the rules require some orbital adjustments to be made which, however, do not violate the basic premise that the nodal properties of the FMO always determine the outcome.[40] As examples we illustrate (in Figure 12) three such cases of interest below:

(35) Woodward, R. B.; Hoffmann, R. *The Conservation of Orbital Symmetry*; Academic Press Inc.: New York, 1970; Chapter 7, pp 114–140. We thank one of the reviewers for pointing out the contrasting predictions of the present symmetry rules for radical cations with those for closed-shell molecules.

(36) Clark, T. *J. Am. Chem. Soc.* **1987**, *109*, 6838.

(37) Bernardi, F.; Robb, M. A.; Schlegel, H. B.; Tonachini, G. *J. Am. Chem. Soc.* **1984**, *106*, 1198.

(38) Bauld, N. L. *Tetrahedron* **1989**, *45*, 5307.

(39) Williams, F. *J. Chem. Soc., Faraday Trans.* **1994**, *90*, 1681.

(40) Fukui, K.; *Acc. Chem. Res.* **1971**, *4*, 57.

Scheme 2. Thermally (Solid Lines) and Photochemically (Dashed Lines) Allowed H-Shifts Connecting Various DHP$^{\bullet+}$ Isomers

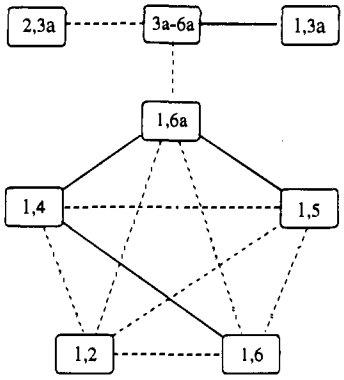

(a) In the LUMO of 1,6a-DHP$^{\bullet+}$ the three nodes are lined up across the three central π-bonds, whereas two of these nodes are usually situated on the terminal π-bonds. Such changes may occur in the course of a reaction as long as the number of nodes (which ultimately determines the character of the MO) is maintained.

(b) In the photochemical transformation from 1,4- to 1,5-DHP$^{\bullet+}$, the *incipient* HOMO has a node bisecting the C2−C3 bond although any realistic MO calculation shows that this node should bisect the C3−C3a bond, as shown in the adjusted HOMO. Likewise, the *incipient* LUMO of 1,5-DHP$^{\bullet+}$ possesses a node bisecting the C3−C3a bond, whereas this is shifted to the C2-C3 bond in the adjusted LUMO.

(c) A similar adjustment is required to convert the incipient LUMO of 1,4-DHP$^{\bullet+}$ (as formed in the H-shift from the 1,6a-tautomer) to the realistic form which is represented in Figure 12. Thus, one should always redraw the reactant MOs in a realistic fashion before proceeding to discuss ensuing steps.

Systematic application of these selection rules to the interconversions between all DHP$^{\bullet+}$ isomers involved in the present study results in Scheme 2 where full lines denote thermally allowed and dashed lines photochemically allowed H-shifts.

This scheme allows a complete discussion of all H-shifts identified (or postulated) on the basis of the experimental observations reported in the present study. Firstly, we note that the starting 3a,6a-DHP$^{\bullet+}$ can only give three different products. One of these (1,3a) may be formed thermally, but this reaction is endothermic and will therefore not occur (cf. section 3e). Of the other two, which require electronic excitation, the one leading to 1,6a is more likely to occur because the energy of the light used to bleach the reactant (635 nm corresponding to 2 eV) suffices barely to cover the endothermicity of the reaction leading to the very unstable 2,3a isomer.

On the other hand, 1,6a-DHP$^{\bullet+}$ can decay via thermally allowed processes to either 1,5- or 1,4-DHP$^{\bullet+}$. Again, the former process is predicted to be endothermic at the ROMP2 level which explains the exclusive formation of 1,4-DHP$^{\bullet+}$. On the other hand, we need to explain why 1,6a- appears to decay spontaneously to 1,4-DHP$^{\bullet+}$ when formed from 3a,6a- and *not* when formed from 1,5-DHP$^{\bullet+}$. This may be due to the fact that in the first case, the product cation is endowed with more excess energy (2 eV from the light used to excite 3a,6a-DHP$^{\bullet+}$ plus 0.17 eV from the exothermicity of the process) than in the latter case (1.5 eV from the light used to excite 1,5-DHP$^{\bullet+}$, the reaction is nearly thermoneutral) which is available to surmount thermal activation barriers.

It is also interesting to note that the 1,5 to 1,6-DHP$^{\bullet+}$ conversion does not proceed thermally (although it should be slightly exothermic), but by photoexcitation, in agreement with the orbital symmetry predictions. Conversely, the back-transformation of 1,6- to 1,4-DHP$^{\bullet+}$ may be interpreted as a likely thermal reaction driven by the energy released on internal conversion of photoexcited 1,6-DHP$^{\bullet+}$.

Scheme 3. Interconversions between DHP$^{\bullet+}$ Tautomers Observed in the Present Study

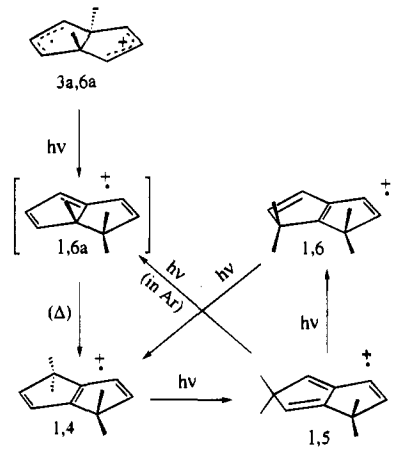

Finally, the formation of (small quantities of) 1,6- on bleaching of 1,4-DHP$^{\bullet+}$ could be due to a secondary photochemical reaction from 1,5-DHP$^{\bullet+}$ (which also absorbs at 400 nm, cf. Section b) because although the direct pathway linking the 1,4- and the 1,6-species is thermally allowed, this process is endothermic in the direction of 1,6-formation. Finally, it is interesting to note that 1,2-DHP$^{\bullet+}$ is predicted to be thermally stable since all H-shifts leading to products of similar stability require electronic excitation.

Summary

We have investigated the complete photochemistry of the radical cation from the bisallylic dihydropentalene, bicyclo-[3.3.0]octa-2,6-diene-4,8-diyl, in Freon and argon matrices by means of electronic absorption and electron spin resonance spectroscopy. Thereby we found that this species undergoes a series of hydrogen shifts to provide successively four of the remaining nine DHP$^{\bullet+}$ isomers according to Scheme 3.

Two of these photoproducts (1,4- and 1,5-DHP$^{\bullet+}$) as well as 1,2-DHP$^{\bullet+}$ were prepared independently from the corresponding neutral DHPs. Their electronic structure is discussed on the basis of photoelectron and electronic absorption spectra. Those are interpreted by means of INDO/S calculations which serve to show that several features of the electronic structure of these novel polyenic cations are unprecedented.

The observed H-shifts are rationalized on the basis of a FMO-based set of rules for sigmatropic rearrangements in radical ions. The structures of all stable neutral and ionic DHP isomers were calculated at the 6-31G*/(RO)HF level and their relative energies evaluated at these geometries by (RO)MP2 calculations. The latter results serve to discuss relaxation energies of the cations observed by PES and the feasiblity of different thermally allowed H-shifts in the cations.

Acknowledgment. The present work has been supported by the Swiss National Science Foundation (Grant No. 2028 040398.94) and by the Division of Chemical Sciences, Office of Basic Energy Sciences, U.S. Department of Energy (Grant No. DE-FG05-88ER13852). Thanks are due to Dr. S. Dai and Mr. R. S. Pappas for help with some preliminary computations of hyperfine couplings and to Dr. W. Tang for technical assistance.

JA9508535